

1 **Preparation of chitosan grafted graphite composite for sensitive detection of dopamine in**  
2 **biological samples**

3 Selvakumar Palanisamy<sup>1</sup>, Kokulnathan Thangavelu<sup>1</sup>, Shen-Ming Chen<sup>\*1</sup>, P. Gnanaprakasam<sup>2</sup>,  
4 Vijayalakshmi Velusamy<sup>3</sup>, Xiao-Heng Liu<sup>4\*\*</sup>

5 <sup>1</sup>Electroanalysis and Bioelectrochemistry Lab, Department of Chemical Engineering and  
6 Biotechnology, National Taipei University of Technology, No.1, Section 3, Chung-Hsiao East  
7 Road, Taipei 106, Taiwan (R.O.C).

8 <sup>2</sup>Department of Nanoscience and Nanotechnology, Karunya University, Coimbatore 64114, India  
9 Corresponding author. Tel: +886 2270 17147; fax: +886 2270 25238.

10 <sup>3</sup>Division of Electrical and Electronic Engineering, School of Engineering, Manchester  
11 Metropolitan University, Manchester – M1 5GD, United Kingdom.

12 <sup>4</sup>Key Laboratory of Education Ministry for Soft Chemistry and Functional Materials, Nanjing  
13 University of Science and Technology, Nanjing 210094, China

14

15 Corresponding author. Tel: +886 2270 17147; fax: +886 2270 25238.

16 \*E-mail address: [smchen78@ms15.hinet.net](mailto:smchen78@ms15.hinet.net) (S.M. Chen); [xhliu@mail.njust.edu.cn](mailto:xhliu@mail.njust.edu.cn) (X.H. Liu)

17

18

19 **Abstract**

20           The accurate detection of dopamine (DA) levels in biological samples such as human  
21 serum and urine samples are essential indicators in medical diagnostics. In this work, we describe  
22 the preparation of chitosan (CS) biopolymer grafted graphite (GR) composite for the sensitive and  
23 lower potential detection of DA in its sub micromolar levels. The composite modified electrode  
24 has been used for the detection of DA in biological samples such as human serum and urine  
25 samples. The GR-CS composite modified electrode shows 6 folds enhanced oxidation peak current  
26 response with low potential for the detection of DA than that of electrodes modified with bare, GR  
27 and CS discretely. Under optimum conditions, the fabricated GR-CS composite modified electrode  
28 shows the DPV response of DA in the linear response ranging from 0.03 to 20.06  $\mu\text{M}$ . The  
29 detection limit and sensitivity of the sensor was estimated as 0.0045  $\mu\text{M}$  and 6.06  $\mu\text{A } \mu\text{M}^{-1} \text{ cm}^{-2}$ .

30 **Keywords:** Graphite; chitosan; biopolymer; dopamine; electro-oxidation; differential pulse  
31 voltammetry.

## 32 **1. Introduction**

33 Over the past few decades, the development of biosensors and chemical sensors for the detection  
34 of neurotransmitters has received a great interest due to the vital role in the metabolic system of  
35 mammals (Pradhan et al., 2014; Jackowska and Krysinski, 2013). In particular, dopamine (DA) is  
36 a well-known inhibitory neurotransmitter and plays an important role in the central nervous system  
37 of the human (Nagatsu and Ichinose, 1999). In general, the DA level in the cerebrospinal fluid  
38 (CSF) is in the range between 0.5 to 25 nM (Suominen et al., 2013). Furthermore, the malfunctions  
39 of DA in CSF leads to many diseases such as Parkinsonism, schizophrenia, hypertension and  
40 pheochromocytoma (Ge et al., 2009). Therefore, the levels of DA in blood or urine are essential  
41 indicators in medical diagnostics for the diseases. To date, different analytical techniques have  
42 been utilized for the reliable determination of DA in biological fluids, such as liquid  
43 chromatography (Meng et al., 2000), capillary electrophoresis (Wey and Thormann, 2001), liquid  
44 chromatography coupled with UV detection (Ary and Rona, 2001), calorimetry (Secor and Glass,  
45 2004), native fluorescence detection (Zhang et al., 2000) and electrochemical methods (Raj et al.,  
46 2003; Cabrita et al., 2005). However, the electrochemical methods are simple, rapid, cost-effective  
47 and efficient method for determination of DA than that of available traditional methods  
48 (Pandikumar et al., 2014).

49 In electrochemical DA sensors, the unmodified electrodes such as glassy carbon, graphite  
50 (GR) and screen printed carbon electrodes are not suitable for detection of DA, due to their poor  
51 selectivity, reproducibility, sensitivity and high overpotentials (Ghanbari and Hajheidari, 2015;  
52 Chen and Cha, 1999). Therefore, the carbon materials, metal oxide, metal alloy nanoparticles,  
53 redox and biopolymers modified electrodes have been widely used for the sensitive and selective  
54 detection of DA in lower overpotential (Pandikumar et al., 2014; Mao et al., 2015; Yan et al., 2015;

55 Li et al., 2015; Vasantha and Chen, 2006; Wang et al., 2006). On the other hand, chitosan (CS) is  
56 known non-toxic, highly biodegradable, naturally abundant linear carbohydrate biopolymer and  
57 widely used in the construction of electrochemical sensors and biosensors. Its various potential  
58 applications include, tissue engineering, artificial skin, burn treatment, wound healing, drug  
59 delivery, (Mertins and Dimova, 2013, 29; Rinaudo, 2006; Vusa et al., 2016). Recently, the CS  
60 functionalized graphene oxide and CS grafted graphene and carbon nanotubes have been used for  
61 the sensing of DA among its various applications (Shan et al., 2010; Demirkol and Timur, 2011;  
62 Liu et al., 2012; Wu et al., 2007; Niu et al., 2012). However, most of the reported DA sensors are  
63 based on CS with pristine graphene and or with carbon nanotubes, in which the composites are  
64 prepared by the direct sonication of graphene or carbon nanotubes in CS solution (Liu et al., 2012;  
65 Niu et al., 2012; Liu et al., 2014). More recently, we have reported DA sensor using the  
66 cyclodextrin grafted GR composite, and the resulting electrode has showed comparable  
67 performance over carbon nanomaterials modified electrodes for sensing of DA (Palanisamy et al.,  
68 2016). The motivation of the present work is to fabricate a simple, sensitive and reliable DA sensor  
69 using the CS grafted GR (GR-CS) composite modified electrode. The CS-GR composite can be  
70 easily prepared by sonication of GR and CS in acetic acid for 1 h at room temperature. Fewer  
71 reports have already reported for the preparation of CS grafted expanded GR (Jagiello et al., 2014;  
72 Demitri et al., 2015). However, for the first time we report a potential application of the GR-CS  
73 composite for the electrochemical sensing of DA.

74 In this work, a sensitive and selective DA sensor was developed based on GR-CS  
75 composite modified electrode for the first time. The GR-CS composite modified electrode shows  
76 an enhanced sensitivity with lower oxidation peak potential for DA than that of pristine GR and  
77 CS modified electrodes. In addition, the GR-CS modified electrode shows a superior performance

78 towards the oxidation of DA than graphene-CS composite, due to its strong intercalation of CS on  
79 exfoliated GR sheets. The selectivity and stability of the sensor were studied and discussed in  
80 detail. The practicability of the sensor also been evaluated in biological samples and discussed.

## 81 **2. Experimental**

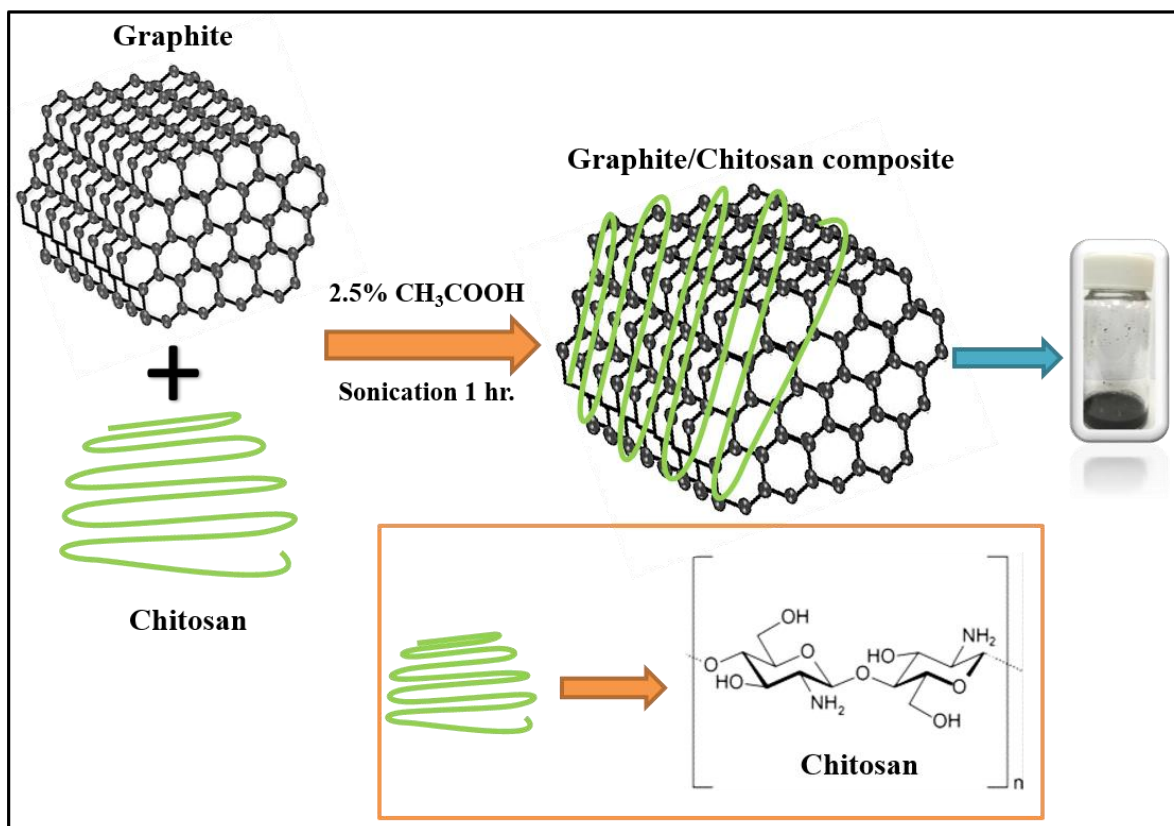
### 82 *2.1. Chemicals*

83 Raw graphite, dopamine and chitosan (from crab shells, minimum 85% deacetylated) were  
84 obtained from Sigma. Uric acid, ascorbic acid and acetic acid were purchased from Aldrich.  
85 Graphene nanopowder (8 nm flakes, product number UR-GNAPHENE) was purchased from  
86 UniRegion Bio-Tech, Taiwan. Human blood serum sample was collected from valley biomedical,  
87 Taiwan product & services, Inc. This study was reviewed and approved by the ethics committee  
88 of Chang-Gung memorial hospital through the contract no. IRB101-5042A3 (Palanisamy et al.,  
89 2016). Human urine sample were collected from the two healthy persons and used for real sample  
90 analysis with their permission. The supporting electrolyte 0.05 M phosphate buffer pH 7 (PBS)  
91 was prepared by using 0.05 M  $\text{Na}_2\text{HPO}_4$  and  $\text{NaH}_2\text{PO}_4$  solutions in doubly distilled water and the  
92 pH were adjusted using 0.1 M  $\text{H}_2\text{SO}_4$  and NaOH. All chemicals used in this study were of  
93 analytical grade and the solutions were prepared using double distilled water without any further  
94 purification.

### 95 *2.2. Apparatus*

96 Cyclic voltammetry (CV) and differential pulse voltammetry (DPV) measurements were  
97 performed by the CHI 750a electrochemical work station. Scanning electron microscopy (SEM)  
98 was performed using Hitachi S-3000 H electron microscope. Raman spectra were recorded using  
99 a Raman spectrometer (Dong Woo 500i, Korea) equipped with a charge-coupled detector. Fourier  
100 transform infrared spectroscopy (FT-IR) was carried out using the Thermo SCIENTIFIC Nicolet

101 iS10 instrument. Conventional three-electrode system was used for the electrochemical  
102 experiments, the glassy carbon electrode (GCE) with geometric surface area of 0.079 cm<sup>2</sup> was  
103 used as a working electrode, a saturated Ag/AgCl as a reference electrode and a platinum electrode  
104 as the auxiliary electrode. All electrochemical measurements were carried out at room temperature  
105 in N<sub>2</sub> atmosphere.



106  
107 **Scheme 1** Schematic representation of preparation of GR-CS composite.

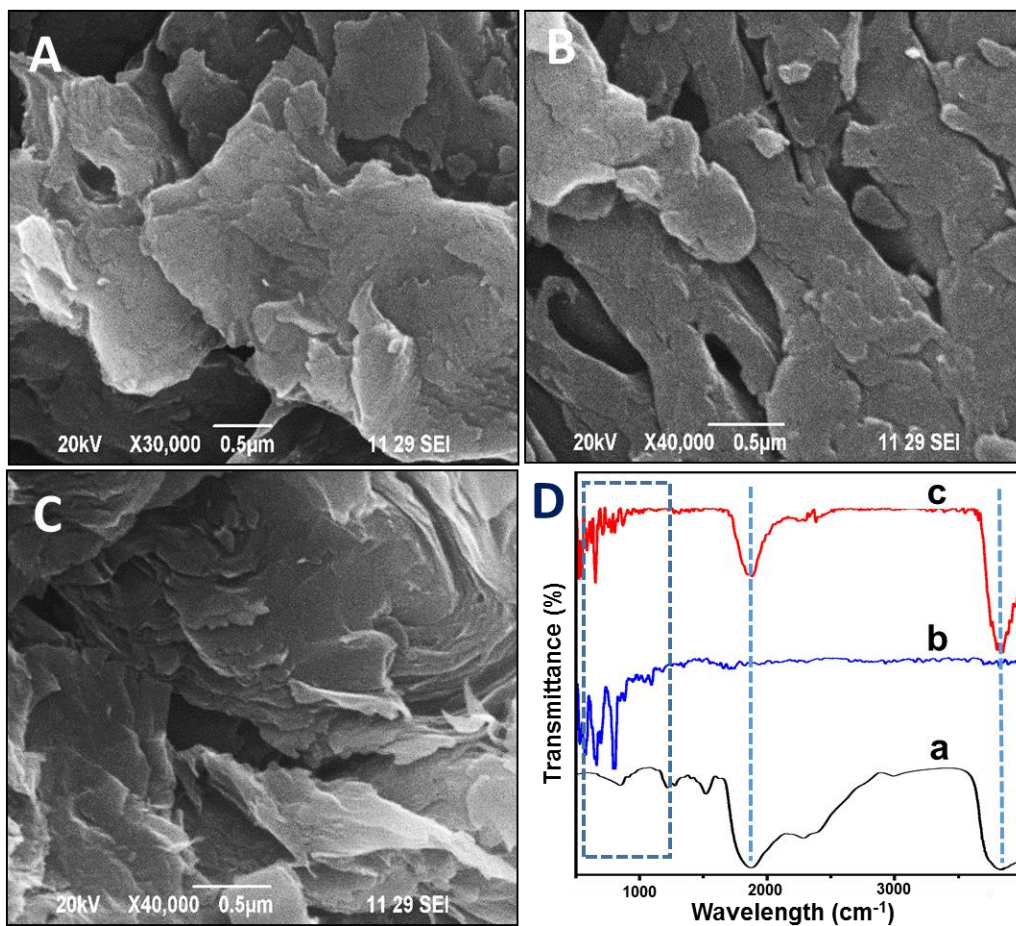
108 *2.3. Preparation of GR-CS composite*

109 To prepare the CS-GR composite, first 15 mg of CS was dissolved in 3 mL of 2.5% acetic acid  
110 with the aid of ultra-sonication. Then, 10 mg GR (2:3 w/w, optimum) was added to the CS solution  
111 and continuously sonicated for 1 h at room temperature. The resulting GR-CS composite was  
112 centrifuged and dried in an air oven. The GR-CS composite was re-dispersed in ethanol and used  
113 for further electrochemical experiments. The preparation of CS-GR composite is shown in **Scheme**

114 1. For controls, GR solution was prepared by dispersing 10 mg of GR in dimethylformamide and  
115 CS solution was prepared by dissolving 15 mg of CS in 2.5% acetic acid. To prepare GR-CS  
116 modified electrode, about 9  $\mu\text{L}$  (optimum) of GR-CS dispersion was drop coated onto pre-cleaned  
117 GCE and dried in room temperature. The GR and CS modified GCEs were independently prepared  
118 by drop coating of 9  $\mu\text{L}$  of GR and CS on pre-cleaned GCE. For comparison with graphene-CS  
119 modified GCE, about 9  $\mu\text{L}$  of the graphene-CS dispersion was drop casted on bare GCE and dried  
120 in an air oven. The graphene-CS dispersion was prepared by dispersing of 10 mg of graphene into  
121 the CS solution (2:3 w/w) with the help of ultrasonication for 1 h at room temperature.

### 122 3. Results and discussion

#### 123 3.1. Characterization of GR-CS composite



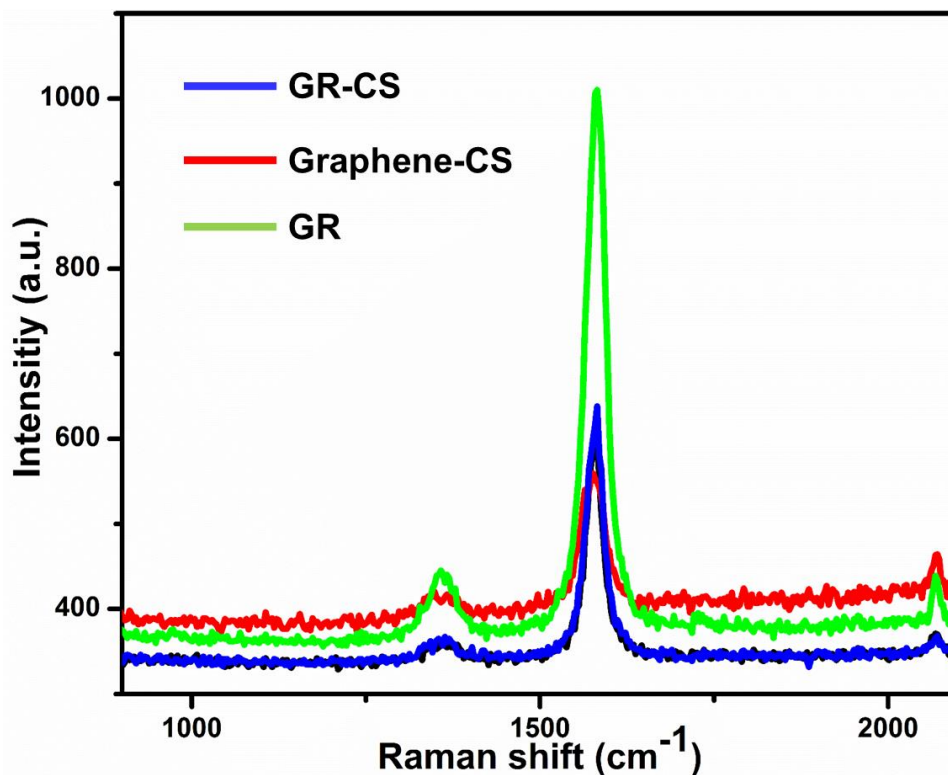
124

125 **Fig. 1** SEM images of (A) pristine GR, B) CS and CS-GR (C). D) FT-IR spectra of CS (a), GR (b)  
126 and GR–CS (c).

127 The surface morphology of GR, CS and GR-CS composite was characterized by SEM. **Fig.**  
128 **1** displays the SEM images of GR (A), CS (B) and GR-CS composite (C). The SEM image of GR  
129 reveals its typical flake sheet morphology with an association of micro graphitic sheets. On the  
130 other hand, the SEM image of CS reveals the uniform, thin and porous nature of CS. The SEM of  
131 GR-CS composite shows that the GR sheets were well separated and grafted with the highly porous  
132 thin film of CS. According to earlier studies, the CS macromolecule is enable to separate graphite  
133 layers and prevent the agglomeration of graphite (Jagiello et al., 2014). Typically, the electron pair  
134 on nitrogen in CS is in protonated form that enable the CS to strongly interact with graphite sheets,  
135 since graphite is known for electron donors (Jagiello et al., 2014). The similar phenomenon has  
136 been reported earlier for CS with graphene and GR. The formation of GR-CS composite was  
137 further confirmed by FTIR. **Fig. 1D** displays the FTIR spectra of CS (a), GR (b) and GR–CS (c).  
138 The FT-IR spectrum of CS depicts characteristic absorption band at 3811 and 3072  $\text{cm}^{-1}$ , is  
139 attributed to the stretching vibrations of –OH. The absorption band at 1525, 1292 and 1114  $\text{cm}^{-1}$ ,  
140 attributed to stretching vibrations of C-O-N and C-O, respectively (Liu et al., 2006). In addition,  
141 two additional bands are observed at 1184 and 841  $\text{cm}^{-1}$ , which is due to the glycosidic bonding  
142 of CS (Jagiello et al., 2014). On the other hand, the FTIR spectrum of GR show the bands at 1369  
143 and 887  $\text{cm}^{-1}$ , which is due to the –CH- bending vibration of GR. The absorption band of CS at  
144 1525  $\text{cm}^{-1}$  for C-O-N was disappeared when mixed with GR, and the absorption band at 1369  $\text{cm}^{-1}$   
145 for C-H stretch was shifted towards 1362  $\text{cm}^{-1}$ . This is possibly due to the strong chemical  
146 interactions between the CS and GR and result into the exfoliation of GR sheets (Gedam et al.,



147 2015). In addition, the observed other absorption bands of GR-CS composite are consistent with  
148 the absorption bands of CS and GR, which confirms that the presence of CS in GR-CS composite.



149  
150 **Fig. 2 A)** Raman spectra of GR-CS (blue line), pristine GR (green line) and graphene-CS (red line).

151 Raman spectroscopy was further employed for characterization of GR and GR-CS  
152 composite and the results were compared with the Raman spectra of graphene-CS composite. **Fig.**  
153 **2** shows the Raman spectra of GR (green profile), GR-CS (blue profile) and graphene-CS (red  
154 line). The G band is corresponding to the first-order scattering of the E<sub>2g</sub> mode in-phase vibration  
155 of the graphite lattice and D band is due to the out-of-plane breathing mode of the sp<sup>2</sup> atoms of  
156 graphite (Jagiello et al., 2014). The Raman spectrum of pure GR shows the weak D and strong G  
157 bands at 1354 and 1579 cm<sup>-1</sup>. The D and G bands of CS grafted GR appears at 1363 and 1583 cm<sup>-1</sup>  
158 <sup>1</sup>, and the G band was greatly reduced after the introduction of CS on GR. In addition, the Raman

159 spectra of GR-CS composite is quite similar to the Raman spectra of graphene-CS composite. The  
160 result indicates that the successful transformation of GR by CS in GR-CS composite.

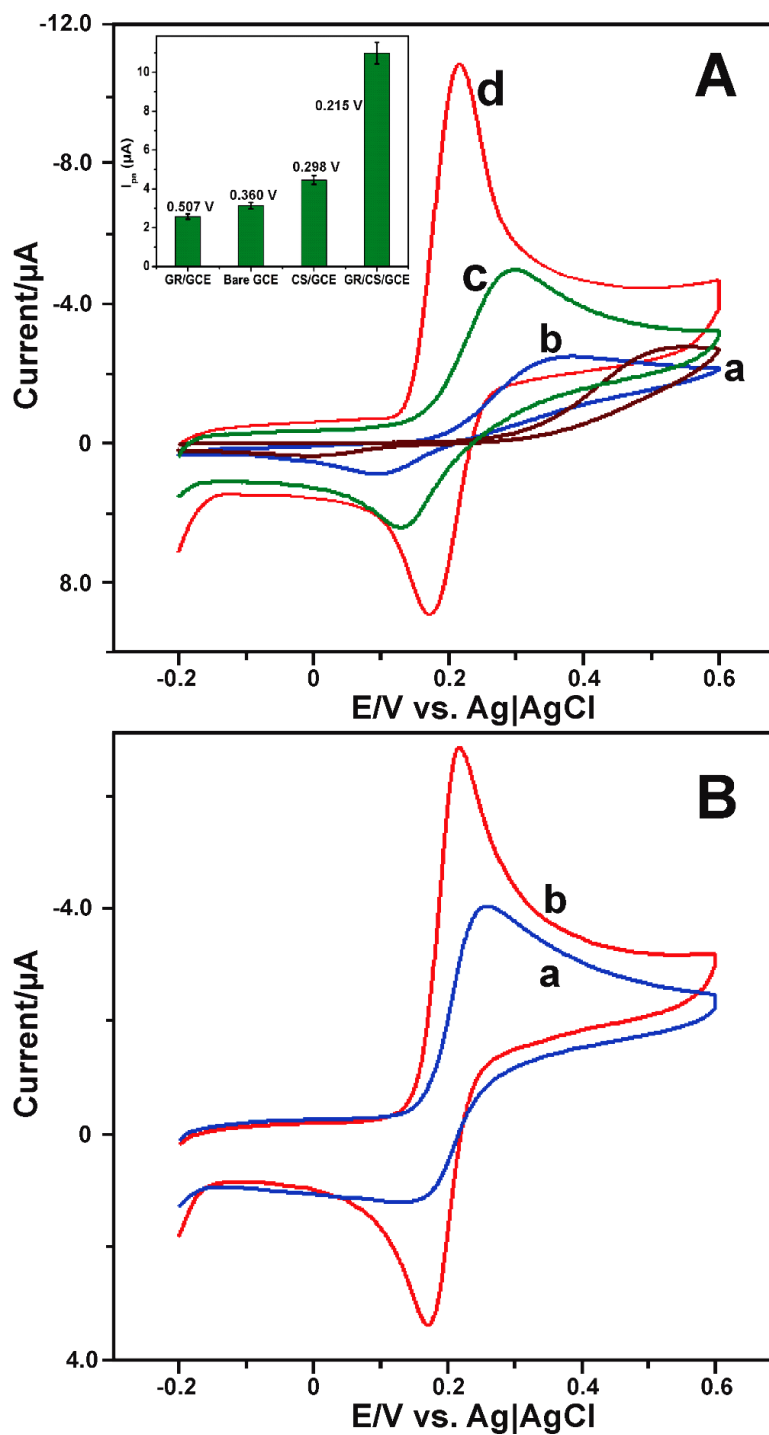
### 161 3.2. Electrochemical behavior of DA

162 CV was used to investigate the electrochemical behaviour of DA at GR-CS composite modified  
163 electrode. **Fig. 3A** shows the CV response of GR (a), bare (b), CS (c) and GR-CS (d) modified  
164 electrodes in 50  $\mu\text{M}$  of DA containing PBS at a scan rate of 50  $\text{mV s}^{-1}$ . The bare and GR modified  
165 electrodes exhibited a weak redox couple for DA and the oxidation peak potential ( $E_{\text{pa}}$ ) of DA was  
166 observed at 0.507 and 0.360 V. The  $E_{\text{pa}}$  of DA was greatly deduced upon the introduction of CS  
167 on GCE, the  $E_{\text{pa}}$  of DA was observed at 0.298 V. In addition, the redox behaviour of DA is greatly  
168 enhanced when compared to the response observed in bare and GR modified electrodes. The result  
169 indicates the efficient electron transfer ability of CS towards the electrode surface. However, GR-  
170 CS composite modified electrode shows a pair of well-defined quasi-reversible redox peak for DA  
171 and the  $E_{\text{pa}}$  of DA was observed at 0.215 V. The observed  $E_{\text{pa}}$  of DA was 0.292, 0.145 and 0.083  
172 V lower than that of GR, bare and CS modified electrodes. Furthermore, the oxidation peak current  
173 ( $I_{\text{pa}}$ ) response of DA at GR-CS composite electrode was 4.2, 3.7 and 2.7 folds higher than the  
174 response observed in GR, bare and CS modified electrodes (**Fig. 3A inset**). The result indicates  
175 that GR-CS composite modified electrode has high electrocatalytic activity towards DA than that  
176 of other modified electrodes.

177 As reported earlier that the protonated form of CS in acidic acid solution could easily  
178 interact with the p electrons in  $\text{sp}^2$  hybrid orbital of GR (Jagiello et al., 2014). In addition, the long  
179 chain of CS is more favourable to interact with each graphitic sheets in GR and result into  
180 exfoliation of GR. The exfoliated GR in GR-CS composite contains high number of basal planes  
181 per volume, while the amount of available edge plane remains the same (Figueiredo-Filho et al.,

182 2013). The large number of basal planes in GR-CS composite and result into the high surface area  
183 and high electrocatalytic activity towards DA. Furthermore, the distinct structure of CS plays an  
184 important role to prevent the accumulation of exfoliated GR in GR-CS composite (Jagiello et al.,  
185 2014). In order to further clarify the catalytic activity, the electrocatalytic behaviour of DA at  
186 GR/CS composite was compared with graphene-CS composite. **Fig. 3B** shows CV responses of  
187 graphene/CS (a) and GR-CS (b) modified electrodes in PBS containing 25  $\mu\text{M}$  of DA in PBS at a  
188 scan rate of 50  $\text{mV s}^{-1}$ . A well-defined quasi redox couple was observed for DA at graphene/CS  
189 composite modified electrode and the oxidation peak of DA was appeared at 0.284 V. However,  
190 the GR-CS modified electrode shows 2 folds enhanced oxidation peak current and lower  
191 overpotential (0.215 V) for detection of DA than that of graphene/CS composite modified  
192 electrode. It is evident from the result that the GR-CS composite has quite higher or similar  
193 electrocatalytic activity to graphene/CS modified electrode.

194 The CS grafted GR composite mostly exists in positive form when the pH was below 5 due  
195 to the protonation of  $-\text{NH}_2$  group of CS (Jiang et al., 2004). While, the protonation of  $-\text{NH}_2$  group  
196 is very low when the pH was more than 6.0, this is more favourable for H-bond interactions  
197 between CS and DA (Jiang et al., 2004). These are the possible reasons for enhanced  
198 electrochemical behavior and lower oxidation potential of DA at GR-CS composite. We have also  
199 investigated the electrochemical behaviour DA at graphene/CS composite and the results are  
200 compared with the response observed at GR-CS composite.



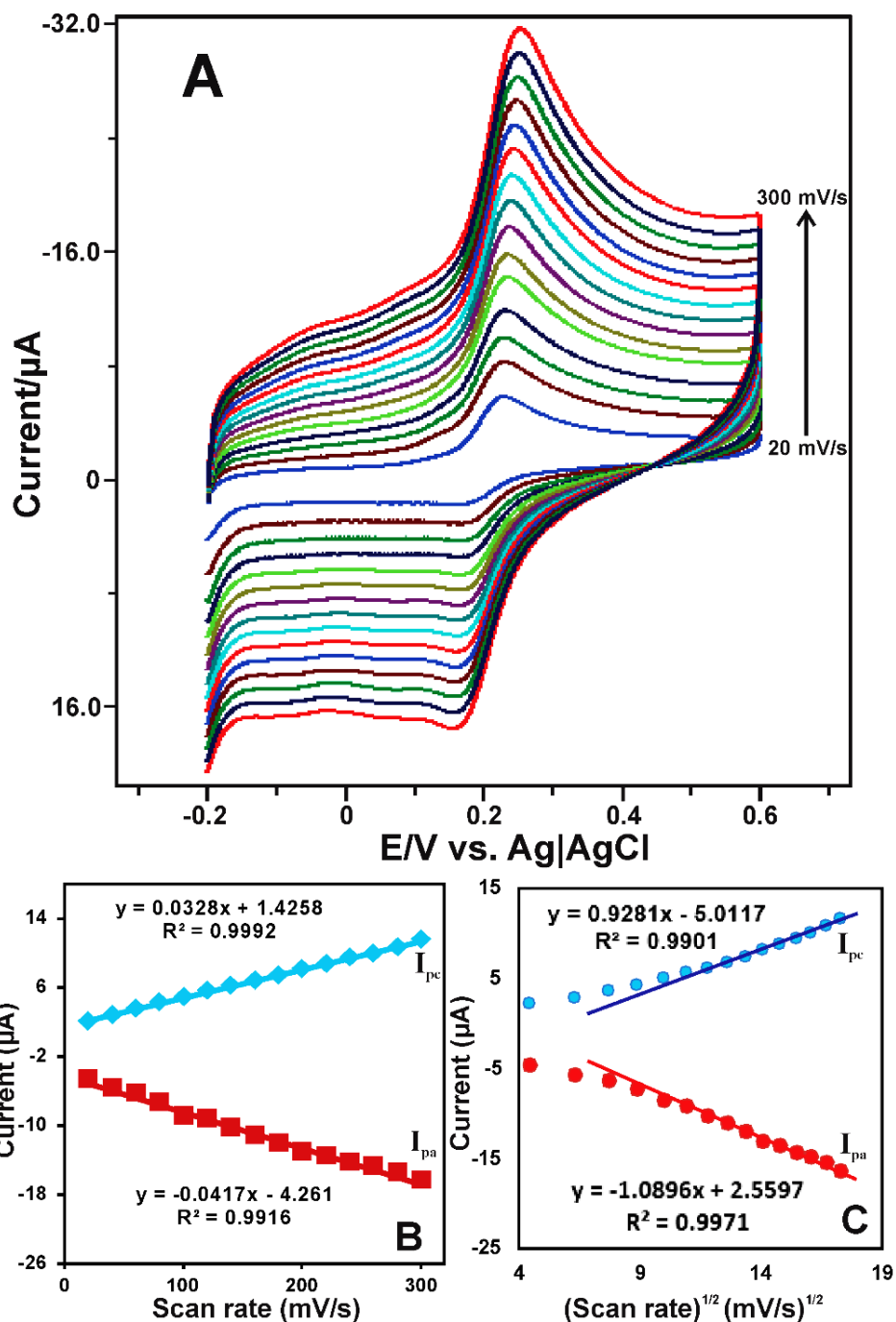
201  
 202 **Fig. 3** A) CV response of the GR (a), bare (b), CS (c) and GR-CS (d) modified GCEs in 50 μM of  
 203 DA containing PBS at a scan rate of 50 mV s<sup>-1</sup>. Inset shows the  $I_{pa}$  and  $E_{pa}$  of DA vs. different  
 204 modified electrodes. B) At the same conditions, CV response of the graphene-CS (a) and GR-CS  
 205 (b) modified GCEs in 25 μM of DA containing PBS at a scan rate of 50 mV s<sup>-1</sup>.

206 *3.3. Optimization*

207 The optimizations studies are more important and it may directly affect the electrochemical  
208 behaviour of DA. Hence, the optimization of GR, CS in GR-CS composite and drop coating  
209 amount of GR-CS composite towards the detection of 50  $\mu\text{M}$  DA was investigated by CV. The  
210 experimental conditions are similar as of in **Fig. 3A**. The optimization results are shown in **Fig.**  
211 **S1A-C**. It can be seen from **Fig. S1A** and **B** that the high sensitivity of DA was observed for 2 and  
212 3 wt% of GR and CS containing GR-CS composite. We have used GR and CS loading as 2 and 3  
213 wt% for optimize the GR and CS. Hence, the 2 and 3 wt% of GR and CS was used for the  
214 preparation of GR-CS composite. In the same manner, 9  $\mu\text{L}$  drop coated GR-CS composite  
215 modified electrode showed a maximum current response for DA than that of other drop coated  
216 electrodes (**Fig. S1C**). Hence, 9  $\mu\text{L}$  drop coated GR-CS composite modified electrode was used as  
217 an optimum quantity for further electrochemical investigations.

218 *3.4. Effect of scan rate and pH*

219 The effect of scan rate on the electrochemical behaviour of 50  $\mu\text{M}$  DA was investigated in PBS by  
220 CV. **Fig. 4A** shows the CV response of GR-CS modified electrode in 50  $\mu\text{M}$  DA containing PBS  
221 at different scan rates from 10 to 300  $\text{mV s}^{-1}$ . It can be seen that the  $I_{\text{pa}}$  and cathodic peak current  
222 ( $I_{\text{pc}}$ ) of DA increases with increasing the scan rate from 10 to 300  $\text{mV s}^{-1}$ .



223  
 224 **Fig. 4** A) CV response obtained at GR-CS modified electrode in the presence of 50  $\mu\text{M}$  DA  
 225 containing PBS at different scan rates from 10 to 300 mV/s. B) Linear dependence of scan rate vs.  
 226  $I_{pa}$ . C) Linear plot of square root of scan rate vs.  $I_{pa}$ .

227 Furthermore,  $I_{pa}$  and  $I_{pc}$  had exhibited a linear relationship with a scan rate from 10 to 300  
 228  $\text{mV s}^{-1}$  (**Fig. 4B**), which indicates that the electrochemical behaviour of DA is controlled by a

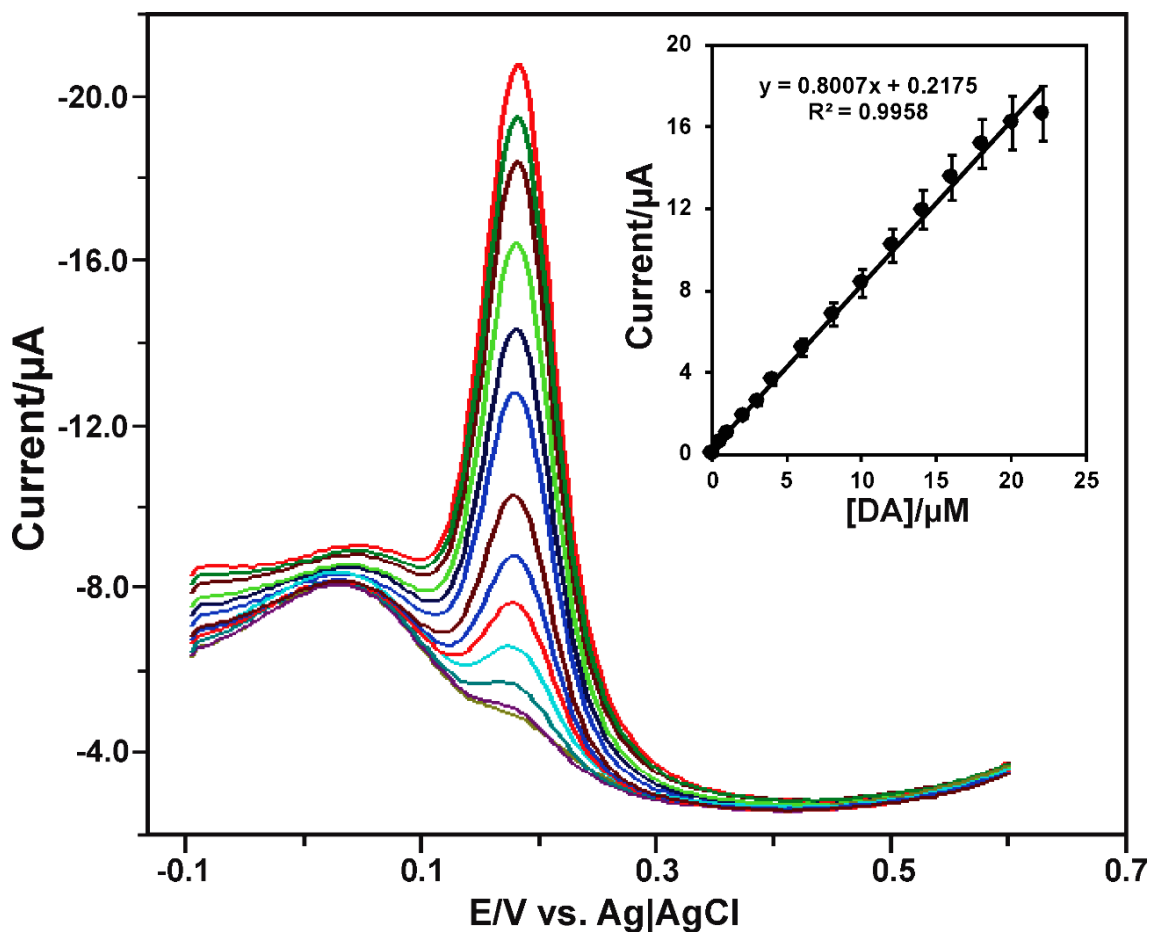
229 typical adsorption-controlled process. However, the ( $I_{pa}$ ) and ( $I_{pc}$ ) are linearly proportional to the  
230 square root of the scan rates from the scan rates from 120 to 300  $\text{mV s}^{-1}$  (**Fig. 4C**), indicating that  
231 electrochemical behaviour of DA is a diffusion controlled process at higher scan rates. The above  
232 result confirms that the electrochemical behaviour of DA at GR-CS composite modified electrode  
233 is controlled by a mixed kinetic process.

234 The electrochemical redox behaviour of 75  $\mu\text{M}$  DA was investigated using the GR-CS  
235 composite modified electrode in different pH solutions by CV. **Fig. S2A** shows the CV response  
236 of GR-CS composite modified electrode in different pH solutions (pH 3, 5, 7, 9 and 11) containing  
237 75  $\mu\text{M}$  of DA at a scan rate of 50  $\text{mV s}^{-1}$ . A well-defined redox couple of DA was observed in  
238 each pH and the  $E_{pa}$  and reduction peak potential ( $E_{pc}$ ) were shifted towards negative and positive  
239 direction upon increasing and decreasing the pH. Furthermore, the  $E_{pa}$  and  $E_{pc}$  of DA had a linear  
240 relationship between the pH from 3 to 11, as shown in **Fig. S2B**. The linear plot was derived  
241 against the formal potential ( $E^{0'} = (E_{pa} + E_{pc})/2$ ) vs. pH and the slope value was found as 58.6  
242  $\text{mV/pH}$  with the correlation coefficient of 0.9854. The observed slope value is close to the  
243 theoretical slope value for an equal number of protons and electrons transferred electrochemical  
244 reaction, as reported previously (Palanisamy et al., 2016). The electrochemical mechanism of DA  
245 at carbon modified electrodes have been well demonstrated and the redox behaviour of DA at GR-  
246 CS composite involves two protons and two electrons coupled electrochemical reaction.

### 247 *3.5. Determination of DA and selectivity of the biosensor*

248 DPV was employed for the electrochemical determination of DA using the GR-CS composite  
249 modified electrode. **Fig. 5** shows the typical DPV response of the GR-CS composite modified  
250 electrode for the absence and presence of additions of different concentration of DA into the PBS.  
251 It can be seen that the GR-CS composite modified electrode did not show any apparent response

252 in the absence of DA. However, a sharp oxidation peak response was observed for the addition of  
253 DA from 0.05 to 22.06  $\mu\text{M}$ . As shown in **Fig. 5 inset**, the GR-CS composite exhibited the response  
254 current of DA was linear over the concentration ranging from 0.03 to 20.06  $\mu\text{M}$  with the correlation  
255 coefficient of 0.9958.



256  
257 **Fig. 5 A)** DPV response of the GR-CS electrode for the additions of different concentration of DA  
258 into the PBS. Inset: Linear relationship of  $I_{pa}$  vs. [DA]. DPV conditions are: sampling width:  
259 0.0167 s; pulse width: 0.05 s; pulse period: 0.2 s; amplitude: 0.05 V; quiet time: 2 s.

260 The sensitivity of the developed sensor was estimated to be  $6.06 \mu\text{A}\mu\text{M}^{-1} \text{cm}^{-2}$  based on the  
261 slope value of the calibration plot. The GR-CS composite modified electrode active surface area  
262 was  $0.12 \text{ cm}^2$ . The limit of detection (LOD) was estimated as  $0.0045 \mu\text{M}$  based on  $S/N=3$ . The



263 fabricated DA sensor exhibited low LOD for DA when compared to sulphonated CS (Vusa et al.,  
264 2016), CS entrapped graphene (Niu et al., 2012; Liu et al., 2014; 36. Weng et al., 2013; Han et al.,  
265 2010; Liu et al., 2011; Wang et al., 2013) and carbon nanotubes modified electrodes (Babaei et al.,  
266 2011), as shown in **Table ST1**. On the other hand, the obtained linear range of our sensor was quite  
267 narrow when compared to the previously reported modified electrodes for the detection of DA. We  
268 have also compared the analytical performance of the present DA sensor with previously reported  
269 tyrosinase based different DA sensors and the comparative results are shown in Table. S2. The  
270 comparison results clear that the fabricated DA sensor shows high sensitivity and comparable LOD  
271 and linear response for the detection of DA (Maciejewska et al., 2011; Zhou et al., 2007; Tsai et al.,  
272 2007; Tembe et al., 2008; Njagi et al., 2008; Min and Yoo, 2009; Njagi et al., Forzani et al., 1995;  
273 Hasebe et al., 1995; Cosnier et al., 1997; Pandey et al., 2001; Ve´drine et al., 2003; Tembe et al.,  
274 2006; Wang, et al., 2010). In addition, the developed DA sensor is less expensive and easy to  
275 prepare when compared with previously enzymatic and non-enzymatic DA sensors (Jackowska and  
276 Krysinski, 2013).

277         The selectivity of the modified electrode is much important for the detection of DA in the  
278 presence of potentially active compounds which are commonly present in biological samples, such  
279 as ascorbic acid (AA) and uric acid (UA). These compounds can potentially interfere the response  
280 of DA on the modified electrode due to their close oxidation potential with DA. Hence, the  
281 selectivity of GR-CS composite modified electrode towards the detection of DA was evaluated in  
282 the presence of AA and UA by DPV. The selectivity results are shown in **Fig. S3**. The experimental  
283 conditions and DPV working parameters are similar as of in **Fig. 5**. The GR-CS composite  
284 modified electrode shows a sharp oxidation peak at 0.194 V for the addition of 1  $\mu$ M DA (a). while,  
285 100  $\mu$ M addition of AA (b) do not show any electrochemical response on the same potential

286 window. In addition, the response current and peak potential of DA was not affected in the  
287 presence of 100  $\mu\text{M}$  AA, which clearly indicates that AA do not have cross reactivity with DA.  
288 On the other hand, the GR-CS composite modified electrode shows a tiny response at 0.384 V for  
289 the presence of 30  $\mu\text{M}$  UA, and the response current of UA increases with the addition of 50, 100  
290 and 200  $\mu\text{M}$  of UA into the PBS. The oxidation peak current response of DA slightly affected in  
291 the presence of UA, while the peak potential of DA unaffected even in the presence of 200  $\mu\text{M}$   
292 UA. The protonation of  $-\text{NH}_2$  group of CS in GR-CS composite is very weak when the pH was  
293 more than 6.0, hence the H-bonding is more favourable towards DA than that of interaction with  
294 UA and AA. This is the possible reasons for high selectivity of the GR-CS composite towards the  
295 detection of DA. The result clearly demonstrates the high selectivity of the fabricated DA sensor.

### 296 *3.6. Determination of DA in biological samples*

297 The practical ability of GR-CS composite modified electrode was evaluated by determination of  
298 DA in biological samples such as human blood serum and urine samples. The standard addition  
299 method was used for the determination of DA in human blood serum and urine samples. The DPV  
300 was used for the determination of DA and the experimental conditions are similar as of in **Fig. 5**.  
301 The human urine samples were diluted 10 times before the DPV measurements. The unknown  
302 concentration of DA was predetermined in DA containing spiked human serum and urine samples  
303 by DPV. Then, the known concentration of DA (2  $\mu\text{M}$ ) containing human blood serum and urine  
304 samples was spiked into the PBS. The obtained recovery results are summarized in **Table ST3**.  
305 The GR-CS composite modified electrode showed the average recovery of DA about 98.3 and  
306 100.5 % DA in the human blood serum and urine samples. The result confirmed that the GR-CS  
307 composite modified electrode could be used for the reliable detection of DA in biological real  
308 samples.

309 The stability of the GR-CS composite modified electrode was examined periodically  
310 towards the detection of 50  $\mu\text{M}$  of DA by CV for 6 days. The GR-CS composite modified electrode  
311 retains 93.6% of the initial current response of DA (figure not shown) after the storage (6 days) in  
312 PBS at 4 °C. The result indicates the good stability of the GR-CS composite modified electrode  
313 towards the detection of DA. The reproducibility and repeatability of the GR-CS composite  
314 modified electrode towards the detection of DA was evaluated by CV. The relative standard  
315 deviation (RSD) of 2.9% was found for 10 measurements of 50  $\mu\text{M}$  DA by single GR-CS  
316 composite modified electrode. The five independently prepared GR-CS composite modified  
317 electrode shows the RSD of 4.3% for the detection of 50  $\mu\text{M}$  DA. The results indicate that GR-CS  
318 composite modified electrode has good repeatability and reproducibility for the detection of DA.

#### 319 **4. Conclusions**

320 We have reported a simple and reliable DA sensor using the GR-CS composite modified  
321 electrode for the first time. The modified electrode showed high catalytic activity and lower  
322 oxidation potential towards the detection of DA, which is attributed to the excellent conductivity  
323 and adsorption property of GR and CS. The as-prepared GR-CS composite modified electrode  
324 shows a high sensitivity, low LOD, appropriate response range and satisfactory stability for the  
325 detection of DA. The GR-CS composite modified electrode has many practical advantages over  
326 the reported nanomaterials modified electrodes for the detection of DA, such as cost-effective,  
327 highly reproducible and can be prepared in short period of time (1 h). The fabricated electrode  
328 showed high selectivity towards DA in the presence of excess addition of AA and UA. The good  
329 recovery of DA in human serum and in urine samples authenticates that the fabricated GR-CS  
330 composite electrode is well suitable for the detection DA for biological and medicinal applications.

#### 331 **Acknowledgments**

332 This project was supported by the Ministry of Science and Technology, Taiwan (Republic of  
333 China).

334

335 **References**

- 336 Ary, K., & Rona, K. 2001. LC determination of morphine and morphine glucuronides in human  
337 plasma by coulometric and UV detection, *J. Pharm. Biomed. Anal.*, 26, 179–187.
- 338 Babaei, A., Babazadeh, M., & Momeni, H.M. 2011. A sensor for simultaneous determination of  
339 dopamine and morphine in biological samples using a multi-walled carbon  
340 nanotube/chitosan composite modified glassy carbon electrode, *Int. J. Electrochem. Sci.*,  
341 6,1382–1395.
- 342 Cabrita, J.F., Abrantes, L.M., & Viana, A.S. 2005. N-Hydroxysuccinimide-terminated self-  
343 assembled monolayers on gold for biomolecules immobilization, *Electrochim. Acta.*, 50,  
344 2117–2124.
- 345 Chen, J., & Cha, C.S. 1999. Detection of dopamine in the presence of a large excess of  
346 ascorbic acid by using the powder microelectrode technique, *J. Electroanal. Chem.*,  
347 463, 93–99.
- 348 Cosnier, S., Innocent, C., Allien, L., Poitry, S., & Tsacopoulos, M. 1997. An electrochemical  
349 method for making enzyme microsensors. application to the detection of dopamine and  
350 glutamate, *Anal. Chem.*, 69, 968–971.
- 351 Demirkol, D.O., & Timur, S. 2011. Chitosan matrices modified with carbon nanotubes for use  
352 in mediated microbial biosensing, *Microchim. Acta.*,173, 537–542.
- 353 Demitri, C., Moscatello, A., Giuri, A., Raucci, M.G., & Corcione, C.E. 2015. Preparation and  
354 characterization of eg-chitosan nanocomposites via direct exfoliation: a green  
355 methodology, *Polymers.*, 7, 2584–2594.

356 Figueiredo-Filho, L.C.S., Brownson, D.A.C., Mingot, M.G., Iniesta, J., Fatibello-Filho, O., &  
357 Banks, C.E. 2013. Exploring the electrochemical performance of graphitic paste electrodes:  
358 graphene vs. graphite, *Analyst.*, 138, 6354–6364.

359 Forzani, E.S., Rivas, G.A., & Solis, V.M. 1995. Amperometric determination of dopamine on  
360 an enzymatically modified carbon paste electrode, *J. Electroanal. Chem.*, 382, 33–40.

361 Ge, B., Tan, Y., Xie, Q., Ma, M., & Yao, S. 2009. Preparation of chitosan–dopamine-multiwalled  
362 carbon nanotubes nanocomposite for electrocatalytic oxidation and sensitive  
363 electroanalysis of NADH, *Sens. Actuators B.*, 137, 547–554.

364 Gedam, A.H., Dongre, R.S., & Bansawal, A.K. 2015. Synthesis and characterization of graphite  
365 doped chitosan composite for batch adsorption of lead (II) ions from aqueous solution, *Adv.  
366 Mater. Lett.*, 6, 59–67.

367 Ghanbari, K., & Hajheidari, N. 2015. ZnO–Cu<sub>2</sub>O/polypyrrole nanocomposite modified  
368 electrode for simultaneous determination of ascorbic acid, dopamine, and uric acid, *Anal.  
369 Biochem.*, 473, 53–62.

370 Han, D., Han, T., Shan, C.S., Ivaska, & A., Niua, L. 2010. Simultaneous determination of  
371 ascorbic acid, dopamine and uric acid with chitosan-graphene modified electrode,  
372 *Electroanalysis.*, 22, 2001–2008.

373 Hasebe, Y., Hirano, T., & Uchiyama, S. 1995. Determination of catecholamines and uric acid in  
374 biological fluids without pretreatment, using chemically amplified biosensors, *Sens.  
375 Actuators, B.*, 24-25, 94–97.

376 Jackowska, K., & Kryszewski, P. 2013. New trends in the electrochemical sensing of dopamine,  
377 *Anal. Bioanal. Chem.*, 405, 3753–3771.

378 Jagiello, J., Judek, J., Zdrojek, M.M., Aksienionek, M., & Lipinska, L. 2014. Production of  
379 graphene composite by direct graphite exfoliation with chitosan, *Mater. Chem. Phys.*, 148,  
380 507–511.

381 Jiang, L., Liu, C., Jiang, L., Peng, Z., & Lu, G. 2004. A chitosan-multiwall carbon nanotube  
382 modified electrode for simultaneous detection of dopamine and ascorbic acid, *Anal. sci.*,  
383 20, 1055–1059.

384 Li, B., Zhou, Y., Wu, W., Liu, M., Mei, S., Zhou, Y., & Jing, T. 2015. Highly selective and  
385 sensitive determination of dopamine by the novel molecularly imprinted poly  
386 (nicotinamide)/CuO nanoparticles modified electrode, *Biosens. Bioelectron.*, 67, 121–128.

387 Liu, B., Lian, H.T., Yin, J.F., & Sun, X.Y. 2012. Dopamine molecularly imprinted  
388 electrochemical sensor based on graphene–chitosan composite, *Electrochim. Acta.*, 75,  
389 108–114.

390 Liu, C., Zhang, J., Yifeng, E., Yue, J., Chen, L., & Li, D. 2014. One-pot synthesis of graphene–  
391 chitosan nanocomposite modified carbon paste electrode for selective determination of  
392 dopamine, *Electron. J. Biotechnol.*, 17, 183–188.

393 Liu, H., Bao, J., Du, Y., Zhou, X., & Kennedy, J.F. 2006. Hydration energy of the 1, 4-bonds of  
394 chitosan and their breakdown by ultrasonic treatment, *Carbohydr. Polym.*, 64, 553–559.

395 Liu, X., Peng, Y., Qua, X., Ai, S., Han, R., & Zhu, X. 2011. Multi-walled carbon nanotube  
396 chitosan/poly(amidoamine)/DNA nanocomposite modified gold electrode for  
397 determination of dopamine and uric acid under coexistence of ascorbic acid, *J. Electroanal.*  
398 *Chem.*, 654, 72–78.

399 Maciejewska, J., Pisareka, K., Bartosiewicz, I., Krysiniski, P., Jackowska, K., & Bieganski, A.  
400 T. 2011. Selective detection of dopamine on poly (indole-5-carboxylic acid)/tyrosinase  
401 Electrode, *Electrochim. Acta.*, 56, 3700-3706.

402 Mao, H., Liang, J., Zhang, H., Pei, Q., Liu, D., Wu, S., Zhang, Y., & Song, X.M. 2015. Poly  
403 (ionic liquids) functionalized polypyrrole/graphene oxide nanosheets for electrochemical  
404 sensor to detect dopamine in the presence of ascorbic acid, *Biosens. Bioelectron.*, 70, 289–  
405 298.

406 Meng, Q. C., Cepeda, M.C., Kramer, T., Zou, H., Matoka, D.J., & Farrar, J. 2000. High-  
407 performance liquid chromatographic determination of morphine and its 3-and 6-  
408 glucuronide metabolites by two-step solid-phase extraction, *J. Chromatogr. B.*, 742, 115–  
409 123.

410 Mertins, O., & Dimova, R. 2013. Insights on the interactions of chitosan with phospholipid  
411 vesicles. part i: effect of polymer deprotonation, *Langmuir.*, 29, 14545–14551.

412 Min, K., & Yoo, Y.J. 2009. Amperometric detection of dopamine based on tyrosinase–SWNTs–  
413 Ppy composite electrode, *Talanta.*, 80, 1007–1011.

414 Nagatsu, T., & Ichinose, H. 1999. Molecular biology of catecholamine-related enzymes in  
415 relation to Parkinson's disease, *Cell. Mol. Neurobiol.*, 19, 57–66.

416 Niu, X., Yang, W., Guo, H., Ren, J., Yang, F., & Gao, J. 2012. A novel and simple strategy for  
417 simultaneous determination of dopamine, uric acid and ascorbic acid based on the stacked  
418 graphene platelet nanofibers/ionic liquids/chitosan modified electrode, *Talanta*, 99, 984–  
419 988.



420 Njagi, J., Chernov, M.M., Leiter, J.C., & Andreescu, S. 2010. Amperometric detection of  
421 dopamine in vivo with an enzyme based carbon fiber microbiosensor, *Anal. Chem.*, 82,  
422 989–996.

423 Njagi, J., Ispas, C., & Andreescu, S. 2008. Mixed ceria-based metal oxides biosensor for  
424 operation in oxygen restrictive environments, *Anal. Chem.*, 80, 7266–7274.

425 Palanisamy, S., Sakthinathan, S., Chen, S.M., Thirumalraj, B., Wu, T.H., Lou, B.S., & Liu, X.  
426 2016. Preparation of  $\beta$ -cyclodextrin entrapped graphite composite for sensitive detection  
427 of dopamine, *Carbohydr.Polym.*, 135, 267–273.

428 Pandey, P.C., Upadhyay, S., Tiwari, I., Singh, G & Tripathi, V.S. 2001. A novel ferrocene  
429 encapsulated palladium–linked ormosil-based electrocatalytic dopamine sensor, *Sens.*  
430 *Actuators, B.*, 75, 48–55.

431 Pandikumar, B., How, G.T.S., See, T.P., Omar, F.S., Jayabal, S., Kamali, K.Z., Yusoff, N., Jamil,  
432 A., Ramaraj, R., John, S.A., Lim, H.N., & Huang, N.M. 2014. Graphene and its  
433 nanocomposite material based electrochemical sensor platform for dopamine, *RSC Adv.*,  
434 4, 63296–63323.

435 Pradhan, T., Jung, H.S., Jang, J.H., Kim, T.W., Kang, C., & Kim, J.S. 2014. Chemical sensing  
436 of neurotransmitters, *Chem. Soc. Rev.*, 43, 4684–4713.

437 Raj, C. R., Okajima, T., & Ohsaka, T.J. 2003. Gold nanoparticle arrays for the voltammetric  
438 sensing of dopamine, *Electroanal. Chem.*, 543, 127–133.

439 Rinaudo, M. 2006. Chitin and chitosan: properties and applications, *Prog. Polym. Sci.*, 31, 603–  
440 632.

441 Secor, K.E., & Glass, T.E. 2004. Selective amine recognition: development of a chemosensor  
442 for dopamine and norepinephrine, *Org. Lett.*, 6, 3727–3730.

443 Shan, C., Yang, H., Han, D., Zhang, Q., Ivaska, A., & Niu, L. 2010. Graphene/AuNPs/chitosan  
444 nanocomposites film for glucose biosensing, *Biosens.Bioelectron.*, 25, 1070–1074.

445 Suominen, T., Uutela, P., Ketola, R.A., Bergquist, T., Hillered, L., Finel, M., Zhang, H., Laakso,  
446 A., & Kostianen, R. 2013. Determination of serotonin and dopamine metabolites in human  
447 brain microdialysis and cerebrospinal fluid samples by UPLC-MS/MS: discovery of intact  
448 glucuronide and sulfate conjugates, *PLoS One.*, 8, e68007.

449 Tembe, S., Karve, M., Inamdar, S., Haram, S., Melo, J., & D'Souza, S.F. 2006. Development of  
450 electrochemical biosensor based on tyrosinase immobilized in composite biopolymeric  
451 film, *Anal. Biochem.*, 349, 72–77.

452 Tembe, S., Kubal, B.S., Karve, M., & D'Souza, S.F. 2008. Glutaraldehyde activated eggshell  
453 membrane for immobilization of tyrosinase from *amorphophallus companulatus*:  
454 Application in construction of electrochemical biosensor for dopamine, *Anal. Chim. Acta.*,  
455 612, 212–217.

456 Tsai, Y.C., & Chiu, C.C. 2007. Amperometric biosensors based on multiwalled carbon nanotube-  
457 nafion-tyrosinase nanobiocomposites for the determination of phenolic compounds, *Sens.*  
458 *Actuators, B.*, 125, 10–16.

459 Vasantha, V.S., & Chen, S.M. 2006. Electrocatalysis and simultaneous detection of dopamine  
460 and ascorbic acid using poly (3, 4-ethylenedioxy) thiophene film modified electrodes, *J.*  
461 *Electroanal. Chem.*, 592, 77–87.

462 Ve´drine, C., Fabiano, S., & Minh, C.T. 2003. Amperometric tyrosinase based biosensor using  
463 an electrogenerated polythiophene film as an entrapment support, *Talanta.*, 59, 535–544.

464 Vusa, C.S.R., Manju, V., Aneesh, K., Berchmans, S., & Palaniappan, A. 2016. Tailored  
465 interfacial architecture of chitosan modified glassy carbon electrodes facilitating selective,  
466 nanomolar detection of dopamine, *RSC Adv.*, 6, 4818–4825.

467 Wang, H.S., Li, T.H., Jia, W.L., & Xu, H.Y. 2006. Highly selective and sensitive determination  
468 of dopamine using a nafion/carbon nanotubes coated poly(3-methylthiophene) modified  
469 electrode, *Biosens. Bioelectron.*, 22, 664–669.

470 Wang, X., Wu, M., Tang, W., Zhu, Y., Wang, L., Wang, Q., He, P., & Fang, Y. 2013.  
471 Simultaneous electrochemical determination of ascorbic acid, dopamine and uric acid  
472 using a palladium nanoparticle/graphene/chitosan modified electrode, *J. Electroanal.*  
473 *Chem.*, 695, 10–16.

474 Wang, Y., Zhang, X., Chen, Y., Xu, H., Tan, Y., & Wang, S. 2010. Detection of dopamine based  
475 on tyrosinase-Fe<sub>3</sub>O<sub>4</sub> nanoparticles-chitosan nanocomposite biosensor, *Am. J. Biomed. Sci.*,  
476 2(3), 209–216.

477 Weng, X., Cao, Q., Liang, L., Chen, J., You, C., Ruan, Y., Lin, H., & Wu, L. 2013. Simultaneous  
478 determination of dopamine and uric acid using layer-by-layer graphene and chitosan  
479 assembled multilayer films, *Talanta.*, 117, 359–365.

480 Wey, A.B., & Thormann, W. 2001. Capillary electrophoresis–electrospray ionization ion trap  
481 mass spectrometry for analysis and confirmation testing of morphine and related  
482 compounds in urine, *J. Chromatogr. A.*, 916, 225–238.

483 Wu, Z., Feng, W., Feng, Y., Liu, Q, Xu, X, Sekino, T, Fujii, A., & Ozaki, M. 2007. Preparation  
484 and characterization of chitosan-grafted multiwalled carbon nanotubes and their  
485 electrochemical properties, *Carbon.*, 45, 1212–1218.

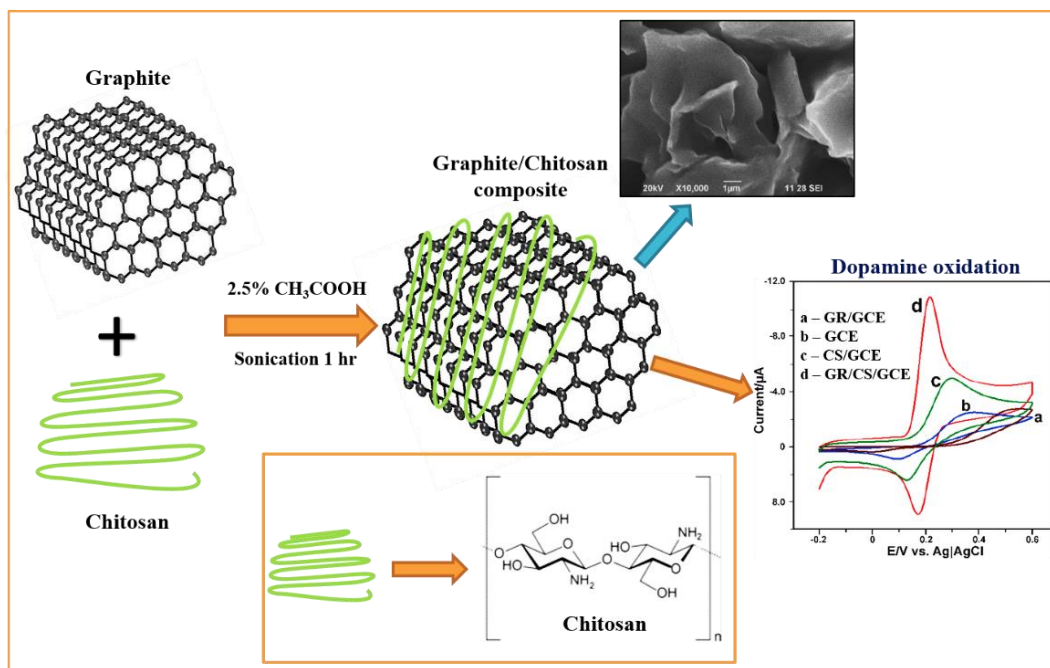
486 Yan, Y., Liu, Q., Du, X., Qian, J., Mao, H., & Wang, K. 2015. Visible light photoelectrochemical  
487 sensor for ultrasensitive determination of dopamine based on synergistic effect of graphene  
488 quantum dots and TiO<sub>2</sub> nanoparticles, *Anal. Chim. Acta.*, 853, 258–264.

489 Zhang, X.X., Li, J., Gao, J., Sun, L., & Chang, W.B. 2000. Determination of morphine by  
490 capillary electrophoresis immunoassay in thermally reversible hydrogel-modified buffer  
491 and laser-induced fluorescence detection, *J. Chromatogr. A*, 895, 1–7.

492 Zhou, Y.L., Tian, R.H., & Zhi, J.F. 2007. Amperometric biosensor based on tyrosinase  
493 immobilized on a boron-doped diamond electrode, *Biosens. Bioelectron.*, 22, 822–828.

494

495



497

498